Refractive index engineering with subwavelength gratings for efficient microphotonic couplers and planar waveguide multiplexers

Cheben, Pavel; Bock, Przemek J.; Schmid, Jens H.; Lapointe, Jean; Janz, Siegfried; Xu, Dan-Zia; Densmore, Adam; Delâge, André; Lamontagne, Boris; Hall, Trevor J.

Publisher’s version / Version de l'éditeur:
https://doi.org/10.1364/OL.35.002526
Optics Letters, 35, 15, pp. 2526-2528, 2010-07-20

Refractive index engineering with subwavelength gratings for efficient microphotonic couplers and planar waveguide multiplexers

Pavel Cheben,[1,*] Przemek J. Bock,[2,1] Jens H. Schmid,[1] Jean Lapointe,[1] Siegfried Janz,[1] Dan-Xia Xu,[1] Adam Densmore,[1] André Delâge,[1] Boris Lamontagne,[1] and Trevor J. Hall[2]

[1]*Institute for Microstructural Sciences, National Research Council Canada, K1A 0R6 Ottawa, Canada*

[2]*Centre for Research in Photonics, University of Ottawa, K1N 6N5 Ottawa, Canada*

**Corresponding author: pavel.cheben@nrc.ca*

Received April 23, 2010; revised June 24, 2010; accepted June 25, 2010; posted July 2, 2010 (Doc. ID 127495); published July 20, 2010

We use subwavelength gratings (SWGs) to engineer the refractive index in microphotonic waveguides, including practical components such as input couplers and multiplexer circuits. This technique allows for direct control of the mode confinement by changing the refractive index of a waveguide core over a range as broad as 1.6–3.5 by lithographic patterning. We demonstrate two experimental examples of refractive index engineering, namely, a microphotonic fiber-chip coupler with a coupling loss as small as –0.9 dB and minimal wavelength dependence and a planar waveguide multiplexer with SWG nanostructure, which acts as a slab waveguide for light diffracted by the grating, while at the same time acting as a lateral cladding for the strip waveguide. This yields an operation bandwidth of 170 nm for a device size of only ~160 μm × 100 μm.

OCIS codes: 130.3120, 230.1950, 060.1810.

Diffraction effects are suppressed for waves propagating in materials structured at the subwavelength scale. Subwavelength periodic structures were first used in the late nineteenth century by Hertz, when studying the properties of the newly discovered radio waves with a fine grid of parallel metal wires used as a polarizer. It was not until the 1940s that electromagnetic wave propagation in a medium structured at the subwavelength scale was first studied [1]. Although the subwavelength phenomenon has been known and exploited for many years in free-space optics [2], little has been reported on using subwavelength periodic structures in dielectric optical waveguides [3,4].

Here, we demonstrate using subwavelength grating (SWG) structures for refractive index engineering in microphotonic silicon waveguides. A basic structure that exemplifies the use of refractive index engineering in a waveguide is shown in Fig. 1. This is a nonresonant photonic structure formed by etching a linear periodic array of rectangular segments into a 260-nm-thick single crystal silicon layer of a silicon-on-insulator wafer. A 2-μm-thick bottom oxide (SiO_2) layer separates the waveguide from the underlying silicon substrate. The waveguide core is a composite medium formed by interlacing the high-refractive-index segments with a material of a lower refractive index, which at the same time is used as the cladding material. The refractive index of the core is controlled lithographically by changing the volume fractions of the two materials. By intermixing Si and SU-8 materials at the subwavelength scale, the refractive index range of ~1.6–3.5 can be obtained.

In order to avoid the formation of standing waves due to Bragg scattering and the opening of a band gap near 1550 nm wavelength, we chose the nominal structural period $d = 300$ nm, which is less than a half of the effective wavelength of the waveguide mode λ_{eff}. Indeed, periodic photonic lattices have been investigated to a great extent, but the efforts have almost exclusively focused on photonic crystals with $d \sim \lambda_{\mathrm{eff}}/2$ that have a band gap at the operational frequency range [5]. In such structures, a waveguide is created by introducing a line-defect in a periodic lattice. In contrast to photonic crystal waveguides, the light is confined in our SWG waveguide by total internal reflection, as in conventional index-guided structures.

Figure 1 (inset) shows the dispersion diagram of our periodic SWG waveguide calculated using the MIT photonic bands software. We have determined that the dispersion away from the bandgap resonance matches that of an equivalent strip waveguide with a core index of 2.65. Electron beam lithography was used to define waveguide patterns in hydrogen silsesquioxane resist. The patterns were then transferred into the silicon layer by inductively coupled plasma reactive ion etching. The samples were coated with a 2-μm-thick SU-8 polymer layer (upper cladding) with a refractive index of 1.58. We estimated the

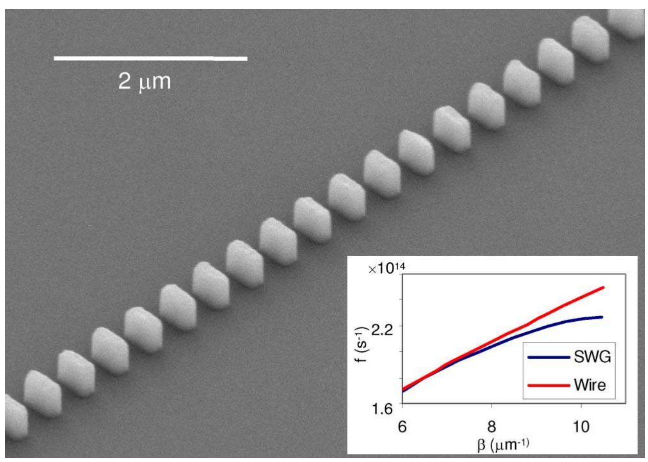

Fig. 1. (Color online) SWG waveguide (SEM image). Inset, dispersion diagrams for SWG and an equivalent strip waveguide with an engineered core refractive index of 2.65 (TE polarization).

0146-9592/10/152526-03$15.00/0

SWG waveguide loss by coupling the light to a set of test waveguides of different lengths varying from 5 to 30 mm, located on the same chip, yielding the propagation loss of –2.1 dB/cm near the 1.55 μm wavelength. Counterintuitive as it may seem that such low loss is achieved for light propagating over a 1 cm distance through more than 33,000 boundaries between high- and low-refractive-index segments, our finding is consistent with the Bloch theory for periodic structures. The group index was measured using Mach–Zehnder interferometer test structures. We have determined a low, polarization independent and almost constant group index of $n_g \sim 1.5$ over the measured wavelength range of $\lambda = 1480$ nm–1580 nm, in agreement with simulation results. A major problem with both conventional and bandgap microphotonic waveguides is their large polarization dependent loss (PDL), and those waveguides are typically used for TE polarization only [5,6]. In our SWG waveguides, the PDL is below 0.5 dB.

We demonstrate the potential of SWG refractive index engineering through the realization of practical functional components. Our SWG coupler, shown in Fig. 2, is designed to reduce the effective index mismatch and the associated loss at the fiber–chip coupling interface. The coupler principle is based on a gradual modification of the waveguide core refractive index and the corresponding mode size transformation by changing the volume fractions of the Si and SU-8 materials that form the composite waveguide core. The microscopic

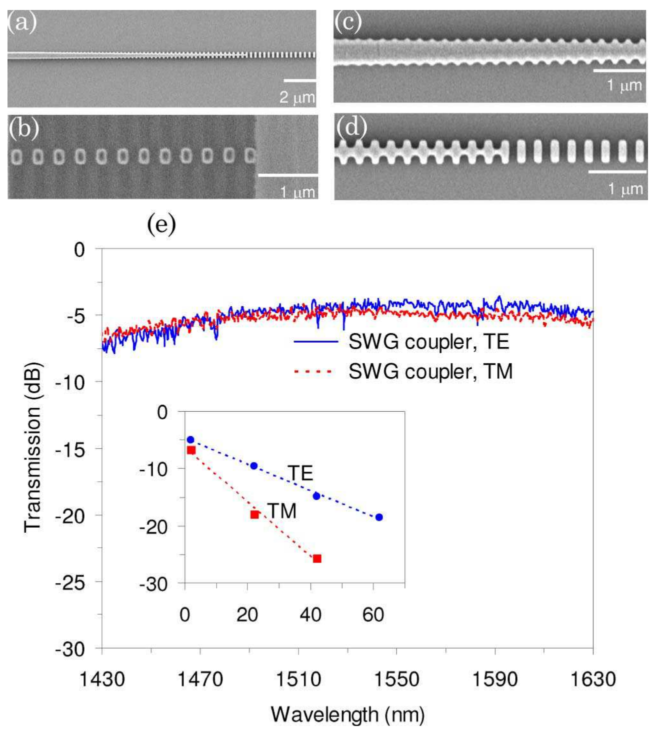

Fig. 2. (Color online) SWG input coupler. (a) SEM image of the coupler. (b) Low-confinement section near the chip edge. (c) High-confinement section near the 450-nm-wide strip waveguide. (d) Intermediate section positioned at $\sim$15 μm from the chip edge. (e) Transmission spectra of the insertion loss of a strip waveguide terminated at both ends with a SWG coupler, for TE (blue) and TM (red) polarizations. The inset shows the intrinsic coupler loss measured on a series of couplers connected back to back.

geometry of the taper was designed such that at one end of the coupler, the effective mode index is matched to a 450-nm-wide silicon strip waveguide for both TE- and TM-like polarizations ($n_{\mathrm{TE}} = 2.51$ and $n_{\mathrm{TM}} = 2.11$), while at the end near the chip facet, it is close to that of an optical fiber ($n \sim 1.5$). We used a lensed single-mode optical fiber with a Gaussian beam waist of 2 μm. Our previous theoretical study allowed us to identify the range of coupler parameters (grating period, chirp, duty ratio, taper length, and tip width) for adiabatic mode transformation with low loss and negligible higher order mode excitation [3]. The fabricated coupler structure is shown in Fig. 2. The grating period is linearly chirped from 400 nm at the chip edge to 200 nm at the junction with the strip waveguide. At the same time, the waveguide width is tapered from 350 nm to 450 nm. Two taper stages with distinct geometries of silicon segments are used to account for different mode confinement in two regions of the coupler. In the first stage [Fig. 2(b)], near the chip edge where the mode is weakly confined, the gaps are fully opened and their lengths linearly decrease from 200 nm to 170 nm. In the second stage [Fig. 2(c)], near the strip waveguide where the mode is highly confined, we used silicon bridging segments to partially fill the gaps, thereby mitigating the loss by making the transition more adiabatic. In this region, the gaps have a constant length (100 nm), and the width of the Si bridging segments linearly increases from 100 nm to 450 nm where the coupler joins the strip waveguide. The two taper stages can also be clearly seen in the intermediate region of the coupler shown in Fig. 2(d).

Transmission spectra of the coupler structure measured using a tunable semiconductor laser are shown in Fig. 2(e), for the wavelength range (1430–1630 nm), which exceeds the full S, C, and L telecom bands. The curves represent the measurements of a 5-mm-long silicon strip waveguide terminated with the SWG couplers at their inputs and outputs, for TE (blue) and TM (red) polarizations. For this structure, a coupling enhancement of $\sim$16 dB is measured, compared to the reference waveguide without the SWG tapers (near $\lambda = 1550$ nm, TE polarization). The insertion loss in Fig. 2(e) includes the coupling loss and the propagation loss in the strip waveguide. The intrinsic coupler loss was determined in an independent measurement using a broadband Er-fiber source on a series of couplers (up to 62) connected back to back as –0.23 dB for TE and –0.47 dB for TM polarizations [see inset of Fig. 2(e)]. The low intrinsic coupler loss is important, as it allows a seamless integration of the silicon strip and SWG waveguides in a photonic circuit. From the measured insertion loss, the waveguide propagation loss, and the coupler intrinsic loss, the total fiber-to-waveguide coupling efficiency was determined as –0.9 dB for TE and –1.2 dB for TM polarizations. To our knowledge, this is the highest efficiency with minimal wavelength and polarization dependence yet reported for a microphotonic coupler [7]. Furthermore, the SWG coupler exhibits a high tolerance to the feature size variations that may arise from limited accuracy of lithography and etching. We found that the coupler loss is negligibly affected by changing the taper tip width from the nominal 350 nm to 300 nm, with loss penalty of less than 0.1 dB for both polarizations. This is a remarkably

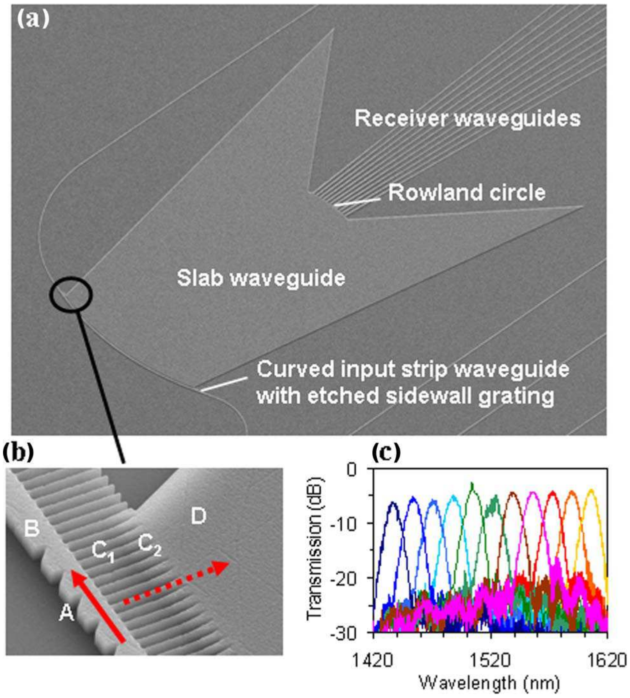

Fig. 3. (Color online) Waveguide grating multiplexer with refractive index engineered SWG interface. (a) Fabricated multiplexer chip. (b) Detailed view showing several grating teeth (A) etched in a sidewall of strip waveguide (B) along with SWG nanostructure (C_1) joining the slab waveguide (D) via a graded-index antireflective SWG interface (C_2). The arrows indicate the light propagation direction in the strip waveguide (solid arrow) and light diffracted (dashed arrow) by the sidewall grating into the slab waveguide region via the SWG interface. (c) Measured multiplexer spectra.

improved fabrication robustness compared to other coupler designs.

As we showed above, in silicon-based waveguides, media with a wide range of intermediate effective indices can be engineered by modifying the volume fractions of the silicon and cladding material. This control of the refractive index in a specific location of a chip is highly desirable for building sophisticated microphotonic circuits, as in the example of the optical multiplexer circuit shown in Fig. 3(a). This new device is only possible using a SWG-engineered nanostructure that provides sufficient optical confinement to make a waveguide, yet have a waveguide boundary that is transparent to light propagating normal to the boundary. In this multiplexer, the light propagating in the curved strip waveguide is diffracted by the grating etched in one of the waveguide sidewalls [Fig. 3(b)]. Curving the waveguide serves the focusing function, so that diffracted light propagates with a convergent wavefront toward the focal region. Different wavelengths are focused at different positions along the focal curve (Rowland circle of radius 80 μm) where they are intercepted by the receiver waveguides. Our previous theoretical study allowed us to calculate design parameters to minimize cross talk and diffraction loss [8]. The subwavelength nanostructure (similar to that reported in [9]) formed in the trench between the strip waveguide and the slab waveguide combiner is shown in Fig. 3(b). The purpose of using the subwavelength trench is twofold: near the strip waveguide an effective material index of $n \sim 2.03$ is created (300 nm SWG pitch, 50% duty ratio, TE polarization). Here, the trench acts as a waveguide for light diffracted by the grating toward the combiner region, while acting as a lateral cladding for the strip waveguide. On the other side of the trench, near the slab waveguide combiner, a triangular SWG structure is used as a graded-index medium to suppress Fresnel reflection for the light propagating from the trench to the slab waveguide. Transmission spectra for 11 channels of the spectrometer are presented in Fig. 3(c). The achieved maximum-to-minimum transmission ratio is as large as ~20 dB, while the loss is approximately −4 dB, allowing for wavelength filtering with a bandwidth of 170 nm. This is the largest wavelength range yet reported for a miniature spectrometer chip. Remarkably, this performance is achieved for a device size of only $\sim 160\ \mu\text{m} \times 100\ \mu\text{m}$.

We demonstrated refractive index engineering in a microphotonic waveguide using SWGs, including implementations in practical components at telecom wavelengths. Our technique circumvents an important limitation in integrated optics, that is, the fixed value of the refractive indices of the constituent materials. These results suggest that SWG waveguides could become important elements for future integrated photonic circuits.

References

1. I. E. Tamm and V. L. Ginzburg, Izv. Akad. Nauk SSSR Ser. Fiz. **7**, 30 (1943).
2. J. N. Mait and W. W. Prather, eds., *Selected Papers on Subwavelength Diffractive Optics*, SPIE Milestone Series, V. Ms 166 (SPIE Press, 2001).
3. P. Cheben, D.-X. Xu, S. Janz, and A. Densmore, Opt. Express **14**, 4695 (2006).
4. J. H. Schmid, P. Cheben, S. Janz, J. Lapointe, E. Post, A. Delâge, A. Densmore, B. Lamontagne, P. Waldron, and D.-X. Xu, Adv. Opt. Technol. **2008**, 685489 (2008).
5. T. J. Krauss, R. M. DeLaRue, and S. Brand, Nature **383**, 699 (1996).
6. F. Xia, L. Sekaric, and Y. Vlasov, Nat. Photon. **1**, 63 (2006).
7. V. R. Almeida, R. R. Panepucci, and M. Lipson, Opt. Lett. **28**, 1302 (2003).
8. P. J. Bock, P. Cheben, A. Delâge, J. H. Schmid, D.-X. Xu, S. Janz, and T. J. Hall, Opt. Express **16**, 17616 (2008).
9. R. Halir, P. Cheben, S. Janz, D.-X. Xu, Í. Molina-Fernández, and J. G. Wangüemert-Pérez, Opt. Lett. **34**, 1408 (2009).